Three Dimensional Ablation Flow Produced by Ultrashort Laser Pulse from Perfectly Flat Target

N. A. Inogamov[1] **V. V. Zhakhovsky**[2], **and V. A. Khokhlov**[1]

[1]L. D. Landau Institute for Theoretical Physics of Russian Academy of Sciences, Russian Federation
[2]Joint Institute for High Temperatures of Russian Academy of Sciences, Russian Federation

Abstract— Surface nanostructuring is one of the most important laser application. Single shot laser action produces fancy three dimensional (3D) patterns on an illuminated boundary. Initially a target is absolutely flat — it possesses a translational two-dimensional symmetry along a boundary. In the paper two sources of the three dimensionality and their interplay are considered. One of them is melting and a nucleation of voids in molten condensed matter as a result of development of random thermal fluctuations, while the another is a tangential gradient of fluence $\nabla_\perp F$ along a boundary. The mechanisms which transfer those sources into the final structures are described below. They start with spallation of a thin pellicle due to a thermomechanical rupture, continue with a capillary interaction inside a foam like transient volume structures mechanically connected with a pellicle, and finish with freezing of those 3D liquid structures back into solid.

1. INTRODUCTION

Laser structuring gives us a variety of useful products such as colorized metals, waterproof surfaces (both obtained first by Vorobyev and Guo), or bio-printing technologies developed by Chichkov and others. There are two limiting examples in the above mentioned applications. In the first of them a laser beam is wide (many optical wavelengths λ in a cross-section), a gradient $\nabla_\perp F$ is negligible, and a random fluctuating nucleation defines structuring. While in the second example a laser spot is close to the diffraction limit and the large gradient $\nabla_\perp F \sim F/\lambda$ dominates the nanobumping and nanojet ejecting. In the second case the gradient suppresses the inevitable (in the spallation process) even smaller (than λ) scale nucleation. In the paper the both examples and their interaction through the gradient modulated nucleation (see Figure 2) are considered.

There are many papers devoted to consideration of an illumination of an initially geometrically 3D objects like the nanoparticles. Or there are papers devoted to analysis of a 3D illumination, e.g., an optical breakdown in transparent media around the waist of a laser beam. Our example with $\nabla_\perp F \sim F/\lambda$ belongs to the cases of the 3D illumination (ablation near a waist). To be geometrically 3D, a radius of surface curvature of an object should be less than or a skin depth, or thermal depth d_T, or λ, here d_T is a thickness of a heated layer created by laser. Those many papers are mentioned because we want better designate our problem with initially absolutely flat target.

A flat boundary excludes the surface plasmone mediated processes connected with interference coupling between an incident plane electromagnetic wave and a boundary perturbation (because perturbations are absent). But influence of plasmons should be included for description of the next laser shots. Below we consider the case of an ultrashort pulse when a nucleation is caused by melting and creation of large tensile stresses in liquid. A thermomechanical stage after such pulse action includes formation of a tensile field and nucleation. It lasts during an acoustic time scale $t_s = d_T/c_s \sim 100\,[\mathrm{nm}]/4\,[\mathrm{km/s}] = 25\,\mathrm{ps}$ for the bulk targets or $t_s = d_f/c_s$ for the thin ($d_f < d_T$) films, here c_s is speed of sound. Motion may be described in the one-dimensional (1D) approximation during this stage, because even in the case $\nabla_\perp F \sim F/\lambda$ a thermal thickness $d_T \sim 100\,\mathrm{nm}$ is an order of magnitude less than a wavelength $\lambda \sim 1000\,\mathrm{nm}$. The 1D approximation means that ablation velocities are directed normally at this stage relative to a surface.

The undersurface nucleation creates a spallation layer, a pellicle, and a foam connecting the pellicle and remnants of a target [1–3]. The transverse velocities comparable with the normal velocities appear in a foam layer during the stage of a 3D nucleation and the stage of the bubble expansion/merging processes in a two-phase mixture. Motions connected with a 3D two-phase capillary turbulence in the bottom of a liquid layer survive for a long (many nanoseconds) times in the case of large fluences when the pellicle disappears and there is a thick hot molten layer. Duration of recrystallization of a thick molten layer increases with its thickness. The bottom velocities at this late stage drop down to the low values $\sim 10\,\mathrm{m/s}$. Thus a long lasting 3D stage follows the short,

fast (10–100 ps) thermomechanical 1D expansion. Similar situation with conversion from 1D to 3D and conversion from the fast motions to the capillary decelerated slow motions takes place in the case of a small heated spot $\nabla_\perp F \sim F/\lambda$ in the regimes when a frozen nanobump is created [4, 5]. This large difference in the time scales allows to simplify problem of nanobump formation, see Section 3.

2. LARGE SPOT AND WEAK MODULATION OF NUCLEATION ACROSS A SPOT

Bulk targets were considered before [1–3]. Here we present new results concerning a gold films on a fused silica substrate. In the simulations a real acoustic impedance of silica is used. For gold a EAM (embedded atom method) potential [6] is employed for molecular dynamics (MD) simulations. MD simulations was supported by the 1D two-temperature hydrodynamics (2T-HD) simulations. A laser pulse has duration 100 fs. We neglect a weak heat conduction of a silica substrate. Thickness of a film is 100 nm. Thickness of a heated layer in a bulk gold is $d_T \approx 140$ nm [7]. Therefore dynamics of our films and the threshold values significantly differ from the case of a thick target.

Simulations describe formation of a cupola and a cavity under the external surface of the cupola (this is the boundary with vacuum) as a result of a thermomechanical expansion of gold after action of a laser beam. The full scale MD simulation with, e.g., 50 microns diameter of a heated spot is outside of the today computer resources, because a corresponding circle of a 100 nm thick film contains 10^{10} atoms. Therefore we have used two approaches. In the first of them we run the 1D MD simulations for a series of absorbed fluences F_{abs} like this was done in papers [1, 2] but for the bulk targets. Results are shown in Figure 1. In the particular simulation box the fluence has been distributed homogeneously along the horizontal lines (one-dimensionality inside the box). But on the horizontal axis of fluences F_{abs} in Figure 1 the boxes are arranged in accordance with their particular value of F_{abs}. Hence we can follow the instant positions of the cupola and cavity boundaries together with the gold/glass contact as functions of the value of local absorbed fluence F_{abs}.

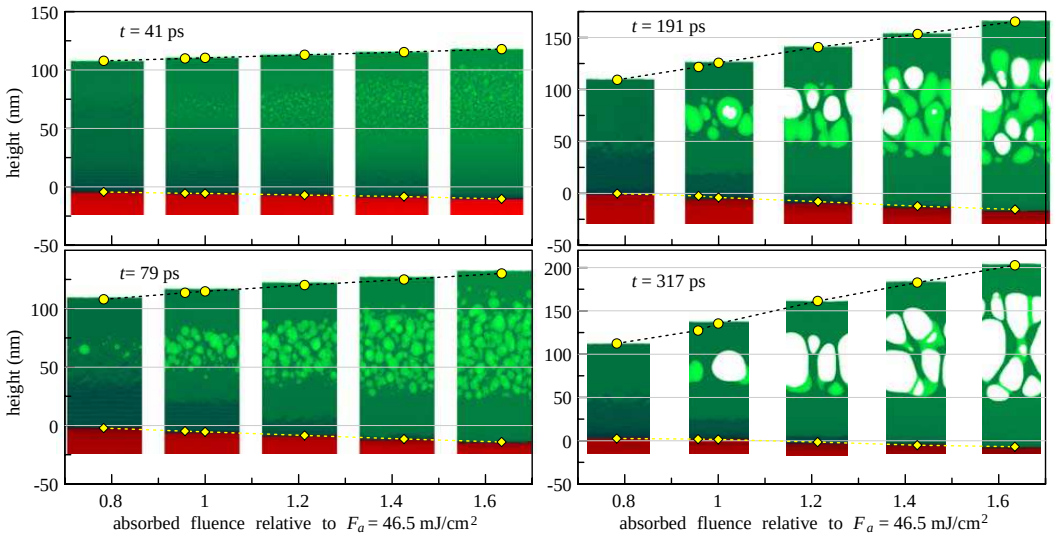

Figure 1: Formation and evolution of a cupola and an internal cavity shown in the approach with a series of the six 1D MD runs. One of those runs is not shown as a particular box, because two runs are too close to each other. Two yellow points inside the second box from the left side correspond to those two runs. It is important to follow the shapes of the four boundaries: a vacuum boundary, an upper boundary of a cavity, a bottom boundary of a cavity, and a contact boundary between gold (green) and glass (red). Molten gold is shown by less dark green. Dark green corresponds to solid. The six yellow points follows instant positions of a vacuum boundary and a contact for the particular values of the relative absorbed fluence plotted at the horizontal axis. The relative fluence is F_{abs}/F_a, where F_a is an ablation threshold. The six runs cover a range 0.78–1.63 of the relative fluences. There are x, y, z axes in the box. The x and y axes correspond to the vertical (normal to target) and horizontal directions. The z axis is perpendicular to the plane of figure. The y-size of the box is 65.4 nm, while the z-size is 16.3 nm. The horizontal three lines mark the initial boundaries and the middle of the gold film. We see that the flow is appreciably asymmetric relative to the middle line, because the glass resists to an expansion of gold, while the vacuum side does not.

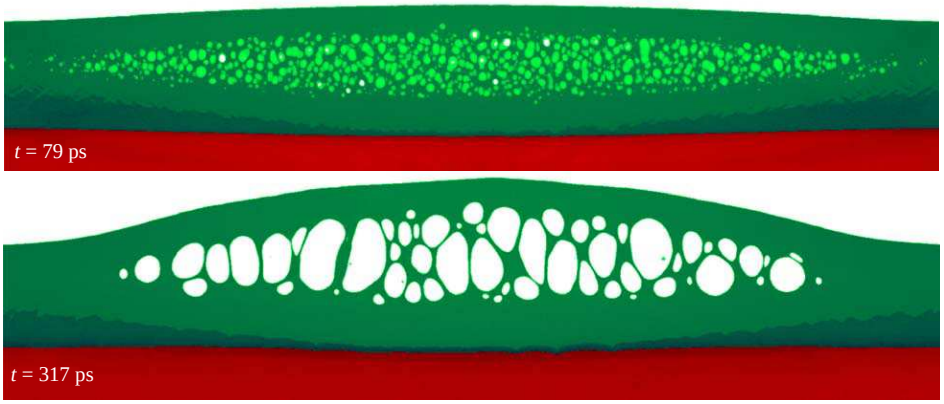

Figure 2: Formation and evolution of a cupola and an internal cavity in the approach with the inhomogeneous illumination $F_{abs}/F_a = 1.4\exp(-y^2/600\,[\mathrm{nm}]^2)$. At the threshold we have $y = 600\sqrt{\ln 1.4} = 348\,\mathrm{nm}$. Interesting, we see that the early nucleation disk is significantly wider in the horizontal direction. This corresponds to the difference between the nucleation and spallation thresholds. The x, y, z axes are defined in previous figure. The y-size of the box is 1000 nm, while the z-size is 8.2 nm.

In the second approach the fluence inside the simulation box has been distributed inhomogeneously $F_{abs}/F_a = 1.4\exp(-y^2/R_L^2)$ along the horizontal lines, here F_a is an ablation threshold relative to an absorbed fluence, R_L is a radius of a laser spot. The Gaussian function describes well the experimental illumination conditions. Evolution of ablation flow in the second approach is shown in Figure 2. Simulation in Figure 2 corresponds to the value $R_L = 0.6$ um. The simulation box in Figure 2 is very wide (1000 nm) for the typical today computer run. Initial thickness of a gold film in Figures 1 and 2 is 100 nm. The glass substrate in Figures 1 and 2 is thick enough to exclude influence of the wave reflected from the bottom boundary of the substrate.

3. SMALL SPOT. FORMATION OF NANOBUMP AND NANOJET

It is very important to develop a true physical picture for the processes taking place during formation of the nanobump under action of the laser beam tightly focused onto thin film, because it is the basis of the LIFT/LIBT technologies (Laser Induced Forward, Backward, Transfer) [4, 5, 8–16]. Those technologies allow precisely manipulate with the nanodroplets made from material of the film. The nanodroplets separate from the jet grown in the apex of the cupola, see Figure 3.

Papers [4, 5] describe how the jet is grown. Dynamic interaction of the laser heated film with substrate repulse the film from substrate. Local velocity v of the film separated from substrate is proportional to the local value of absorbed fluence $v[F_{abs}(y, z)]$. Therefore a fluence distribution defines the shape of the curved surface of the separated thin film. Very different shapes may be produced varying the distributions. Here we consider a Gaussian distribution. It has a maximum in the center. Thus the cupola like (or dome like) shapes appear, see Figure 3.

Inertial mass of matter forming the cupola shell flies away from the substrate. Therefore height of the cupola increases (cupola inflates). Capillary forces decelerate the shell, then the cupola height achieves its maximum and begins to decrease back to substrate [4, 5]. Significant mass concentrates in the axial region due to focusing action of the convex cupola and deceleration. The ratio of surface tension stress per mass is low in the axial region. Therefore capillary force can decelerate the shell but not the axial mass. Thus the axial mass keeps part of its momentum and the axial jet begin to grow, see Figure 3. This physical picture has been developed in papers [4, 5]. The new development presented here corresponds to freezing. Figure 3 shows how the liquid is cooled and how it recrystallizes during its flight.

Paper [17] argue that there are different regimes of motion of the film/substrate system. Transitions between them mainly depend on absorbed fluence F_{abs}, cohesion strength p_{coh} between metal and glass at the contact, and on relative thickness d_f/d_T of a film. There are three regimes divided by two thresholds $0 < F_{contct} < F_{film}$ in the case of a weak contact cohesion. Film oscillates and remains on the substrate in the regime of weak illumination $F < F_{contct}$. The film separates as whole from substrate in the case of moderate fluences $F_{contct} < F < F_{film}$. The evolution shown in Figure 3 corresponds namely to this case. In the high fluence regime $F_{film} < F$ a film breaks inside a film. The part of the film adjoining to the contact remains at the contact. The threshold corre-

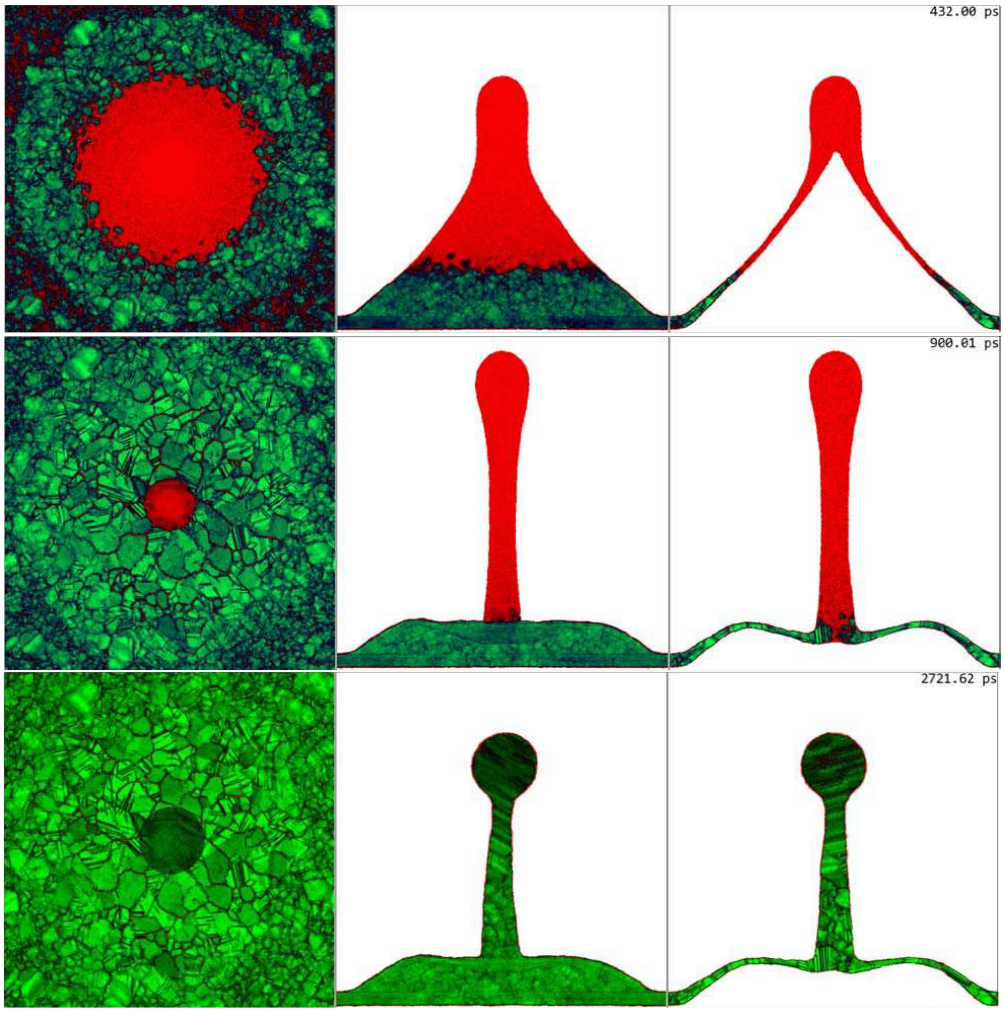

Figure 3: Formation and evolution of the cupola and the internal cavity after separation of the gold film from the silica substrate is shown. Cooling of gold along the film is very significant. Namely this process leads to freezing of liquid gold. Solid is green, liquid is red. The solidified shell is "woven" from a multitude of nanocrystallites. They are transiently deformed during oscillations of the solidifying shell. The liquid is significantly overcooled. Therefore the solidification proceeds not only with crystallization front, but also in the volume of liquid and at the free surface. The side of the computational square shown in the left column is 140 nm. The series of the frames explains how the nanobump with the jet above is formed.

sponding to separation of a film as whole from substrate disappears in the case of strong cohesion. Cohesion of gold to silica is weak, but it becomes much stronger if there is a chromium layer at the contact. Evolution of a film strongly attached to the glass is shown in Figures 1 and 2.

4. CONCLUSION

Above the spallation and 3D foaming in the case when thickness of a film d_f is smaller than a heated depth d_T is considered. Previously foaming in case of a bulk target has been studied [1, 2]. Here we have analyzed how the limited thickness d_f and presence of a substrate influence foaming. We have to emphasize that if the non-conducting substrate works as a thermal wall strongly enlarging time needed for solidification, then the foaming itself will not leads to formation of surface nanostructures after a single shot, because a surface tension will have time to smooth out the roughness created by the foaming together with the decay of foam. Thus cooling properties of the substrate is essential for the thermomechanical surface structuring of metal films (e.g., change glass to crystallin silicon). This is said for the case of large illuminated spot.

In Section 3 the logical picture of physical phenomena leading to formation of the nanobump with jet is presented. Effect of solidification in flight is described.

ACKNOWLEDGMENT

The work has been done under support from the Russian Science Foundation, grant 14-19-01599.

REFERENCES

1. Inogamov, N. A., V. V. Zhakhovskii, S. I. Ashitkov, Y. V. Petrov, M. B. Agranat, et al., "Nanospallation induced by an ultrashort laser pulse," *JETP*, Vol. 107, No. 1, 1–19, 2008.
2. Wu, C. and L. V. Zhigilei, "Microscopic mechanisms of laser spallation and ablation of metal targets from large-scale molecular dynamics simulations," *Appl. Phys. A*, Vol. 114, 11–32, 2014.
3. Inogamov, N., et al., "Ultrafast lasers and solids in highly excited states: Results of hydrodynamics and molecular dynamics simulations," *J. Phys.: Conf. Ser.*, Vol. 510, 012041, 2014.
4. Inogamov, N. and V. Zhakhovskii, "Formation of nanojets and nanodroplets by an ultrashort laser pulse at focusing in the diffraction limit," *JETP Lett.*, Vol. 100, No. 1, 4–10, 2014.
5. Inogamov, N. A., V. V. Zhakhovsky, et al., "Jet formation in spallation of metal film from substrate under action of femtosecond laser pulse," *JETP*, Vol. 120, No. 1, 15–48, 2015.
6. Zhakhovskii, V., et al., "Molecular dynamics simulation of femtosecond ablation and spallation with different interatomic potentials," *Appl. Surf. Sci.*, Vol. 255, No. 24, 9592–9596, 2009.
7. Demaske, B. J., V. V. Zhakhovsky, N. A. Inogamov, and I. I. Oleynik, "Ablation and spallation of gold films irradiated by ultrashort laser pulses," *Phys. Rev. B*, Vol. 82, 064113, 2010.
8. Unger, C., J. Koch, L. Overmeyer, and B. N. Chichkov, "Time-resolved studies of femtosecond-laser induced melt dynamics," *Optics Express*, Vol. 20, No. 22, 24864–24872, 2012.
9. Ivanov, D. S., et al., "Short laser pulse nanostructuring of metals: Direct comparison of molecular dynamics modeling and experiment," *Appl. Phys. A*, Vol. 111, 675–687, 2013.
10. Nakata, Y., N. Miyanaga, and T. Okada, "Topdown femtosecond laser-interference technique for the generation of new nanostructures," *J. Phys.: Conf. Ser.*, Vol. 59, 245–248, 2007.
11. Zywietz, U., et al., "Laser printing of silicon nanoparticles with resonant optical electric and magnetic responses," *Nature Comm.*, Vol. 5, No. 3402, 2014, Doi: 10.1038/ncomms4402.
12. Zywietz, U., C. Reinhardt, A. B. Evlyukhin, et al., "Generation and patterning of Si nanoparticles by femtosecond laser pulses," *Appl. Phys. A*, Vol. 114, No. 1, 45–50, 2014.
13. Ivanov, D. S., B. Rethfeld, et al., "The mechanism of nanobump formation in femtosecond pulse laser nanostructuring of thin metal films," *Appl. Phys. A*, Vol. 92, 791–796, 2008.
14. Emelyanov, V. I., D. A. Zayarniy, et al., "Nanoscale hydrodynamic instability in a molten thin gold film induced by femtosecond laser ablation," *JETP Lett.*, Vol. 99, No. 9, 518–522, 2014.
15. Gubko, M. A., et al., "Enhancement of ultrafast electron photoemission from metallic nanoantennas excited by a femtosecond laser pulse," *Laser Phys. Lett.*, Vol. 11, 065301, 2014.
16. Domke, M., S. Rapp, M. Schmidt, and H. P. Huber, "Ultrafast pump-probe microscopy with high temporal dynamic range," *Optics Express*, Vol. 20, No. 9, 10330–10338, 2012.
17. Inogamov, N., V. Khokhlov, V. Zhakhovsky, et al., "Femtosecond laser ablation of thin films on substrate," *PIERS Proceedings*, Prague, Czech Republic, Jul. 2015.